

## Discovery of MK-1421, a Potent, Selective sstr3 Antagonist, as a Development Candidate for Type 2 Diabetes

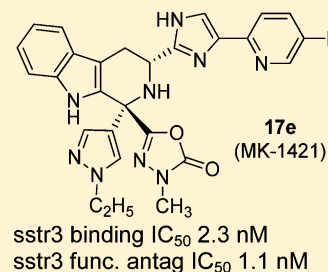
Shrenik K. Shah,<sup>†</sup> Shuwen He,<sup>†</sup> Liangqin Guo,<sup>†</sup> Quang Truong,<sup>†</sup> Hongbo Qi,<sup>†</sup> Wu Du,<sup>†</sup> Zhong Lai,<sup>†</sup> Jian Liu,<sup>†</sup> Tianying Jian,<sup>†</sup> Qingmei Hong,<sup>†</sup> Peter Dobbelaar,<sup>†</sup> Zhixiong Ye,<sup>†</sup> Edward Sherer,<sup>‡</sup> Zhe Feng,<sup>‡</sup> Yang Yu,<sup>†</sup> Frederick Wong,<sup>†</sup> Koppara Samuel,<sup>§</sup> Maria Madiera,<sup>§</sup> Bindhu V. Karanam,<sup>§</sup> Vijay B. Reddy,<sup>§</sup> Stan Mitelman,<sup>§</sup> Sharon X. Tong,<sup>§</sup> Gary G. Chicchi,<sup>||</sup> Kwei-Lan Tsao,<sup>||</sup> Dorina Trusca,<sup>||</sup> Yue Feng,<sup>||</sup> Margaret Wu,<sup>||</sup> Qing Shao,<sup>||</sup> Maria E. Trujillo,<sup>||</sup> George J. Eiermann,<sup>||</sup> Cai Li,<sup>||</sup> Michele Pachanski,<sup>||</sup> Guillermo Fernandez,<sup>⊥</sup> Donald Nelson,<sup>⊥</sup> Patricia Bunting,<sup>⊥</sup> Pierre Morissette,<sup>⊥</sup> Sylvia Volksdorf,<sup>⊥</sup> Janet Kerr,<sup>⊥</sup> Bei B. Zhang,<sup>||</sup> Andrew D. Howard,<sup>||</sup> Yun-Ping Zhou,<sup>||</sup> Alexander Pasternak,<sup>†</sup> Ravi P. Nargund,<sup>†</sup> and William K. Hagmann<sup>\*,†</sup>

<sup>†</sup>Departments of Medicinal Chemistry, <sup>‡</sup>Chemistry Modeling and Infomatics, <sup>§</sup>Drug Metabolism and Pharmacokinetics, and <sup>||</sup>Diabetes Research, Merck Research Laboratories, 2000 Galloping Hill Road, Kenilworth, New Jersey 07033, United States

<sup>⊥</sup>Department of Safety Assessment, Merck Research Laboratories, 770 Sumneytown Pike, West Point, Pennsylvania 19486, United States

### S Supporting Information

**ABSTRACT:** The imidazolyl-tetrahydro- $\beta$ -carboline class of sstr3 antagonists have demonstrated efficacy in a murine model of glucose excursion and may have potential as a treatment for type 2 diabetes. The first candidate in this class caused unacceptable QTc interval prolongation in oral, telemetrized cardiovascular (CV) dogs. Herein, we describe our efforts to identify an acceptable candidate without CV effects. These efforts resulted in the identification of (1*R*,3*R*)-3-(4-(5-fluoropyridin-2-yl)-1*H*-imidazol-2-yl)-1-(1-ethyl-pyrazol-4-yl)-1-(3-methyl-1,3,4-oxadiazol-3*H*-2-one-5-yl)-2,3,4,9-tetrahydro-1*H*- $\beta$ -carboline (**17e**, MK-1421).



**KEYWORDS:** sstr3, antagonist, type 2 diabetes, tetrahydro- $\beta$ -carboline

We recently reported the discovery of a potent, selective sstr3 (somatostatin subtype-3 receptor) antagonist **1** (MK-4256) as a potential treatment for type 2 diabetes.<sup>1</sup> This tetrahydro- $\beta$ -carboline derivative is characterized by excellent sstr3 potency and subtype selectivity, a good pharmacokinetic (PK) profile in preclinical species, and exceptional potency in an oral glucose tolerance test (oGTT) in mice. On the basis of this attractive profile, compound **1** was advanced as a preclinical development candidate. However, in cardiovascular (CV) safety evaluation in dogs, **1** exhibited unexpected potentiation of the QTc interval. Initial studies indicated that the CV effects were not caused by binding to the sstr3 receptor.<sup>2</sup> Nicotinic acid derivative **2** is a potent sstr3 antagonist devoid of ion channel binding that exhibited little to no effects on the QTc interval in dogs, thus providing evidence that the observed cardiovascular effects were likely associated with ion channel binding and not sstr3 (Table 1). Herein, we describe our efforts to identify an acceptable clinical candidate in this class of tetrahydro- $\beta$ -carboline sstr3 antagonists with reduced QTc increase potential.

An initial assessment of the phenyl-imidazolyl-tetrahydro- $\beta$ -carboline structure suggested that it might contain the proposed hERG channel pharmacophore: a basic amine

centered between two broad hydrophobic domains.<sup>3,4</sup> The p*K*<sub>a</sub> of the tetrahydro- $\beta$ -carboline nitrogen would be expected to play an important part in the binding to the ion channel through a putative  $\pi$ -cation interaction.<sup>5</sup>

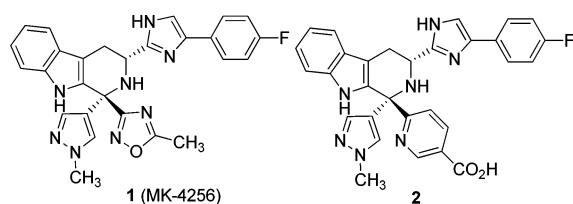
Lowering of the nitrogen p*K*<sub>a</sub> or its replacement was explored through a series of simple analogues (Table 2). These compounds were prepared by methods previously described involving a Pictet–Spengler cyclization of the phenyl imidazolyl tryptamine with the appropriate aldehyde or ketone.<sup>6,7</sup>

The examples in Table 2 should be considered in pairs: compounds **3** and **4** compare the tetrahydro- $\beta$ -carboline nitrogen replaced by carbon. There is a small loss of sstr3 binding, a large loss in receptor antagonism, and a significant gain in hERG binding. Compounds **5** and **6** highlight the effect of oxygen replacement for nitrogen. The large changes observed in all three assays reflect the large structural change of replacing a basic amine with a neutral, polar oxygen. Finally, C-1 substituted analogues **7** and **8** both retain the nitrogen, but

**Received:** December 9, 2014

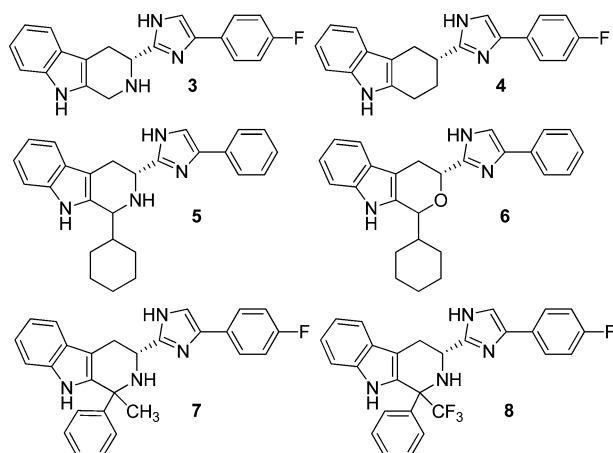
**Accepted:** March 18, 2015

**Published:** March 18, 2015

**Table 1. Binding to h-sstr3 and hERG Channel by Tetrahydro- $\beta$ -carbolines 1 and 2<sup>a</sup>**

	1	2
<b>h-sstr3 binding</b>		
<b>IC<sub>50</sub>, nM (±StD, n)</b>	0.7 (0.2, 50)	7.9 (4.9, 4)
<b>h-sstr3 antagonism</b>		
<b>IC<sub>50</sub>, nM (±StD, n)</b>	0.9 (1.7, 26)	2.4 (0.6, 2)
<b>hERG binding</b>		
<b>IC<sub>50</sub>, μM (n)</b>	1.7 (1)	95.6 (1)
<b>hERG functional, IC<sub>50</sub>, μM (n)</b>	3.4 (1)	26% @ 30 μM

<sup>a</sup>StD = standard deviation; *n* = number of determinations; nd = not determined.

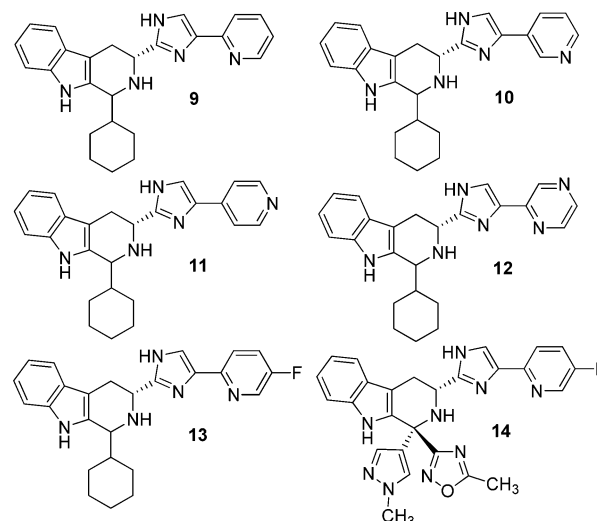
**Table 2. Binding to h-sstr3 and hERG Channel by Modified Tetrahydro- $\beta$ -carboline Analogues<sup>a</sup>**

	<b>h-sstr3 binding IC<sub>50</sub>, nM (±StD, n)</b>	<b>h-sstr3 antag IC<sub>50</sub>, nM (±StD, n)</b>	<b>hERG binding Ki, μM (n)</b>
3	11.4 (7.4, 2)	15.0 (1.7, 2)	0.29 (2)
4	24.9 (7.2, 2)	538.6 (nd, 1)	0.05 (2)
5	0.8 (0.3, 5)	26.1 (nd, 1)	0.08 (2)
6	25.3 (4.6, 2)	156.6 (nd, 1)	0.44 (2)
7	4.6 (-, 1)	15.7 (8.0, 2)	2.87 (1)
8	2.1 (0.3, 2)	13.3 (1.7, 2)	0.72 (1)

<sup>a</sup>StD = standard deviation; *n* = number of determinations; nd = not determined.

the presence of the trifluoromethyl group in 8 would be expected to dramatically lower the p*K*<sub>a</sub> of the nitrogen. sstr3 activities are retained, but there is actually an increase in hERG channel binding. Taken together, the results in Table 2 suggest that a strategy of replacing or attenuating basicity of the tetrahydro- $\beta$ -carboline nitrogen would not be fruitful.

The structure–activity relationship (SAR) of the phenyl-imidazole moiety in 5 was examined for effects on sstr3 and hERG activities (Table 3). Phenyl-imidazoles are reported to

**Table 3. Binding to h-sstr3 and hERG Channel by Heteroaryl-imidazolyl-tetrahydro- $\beta$ -carbolines<sup>a</sup>**

	<b>h-sstr3 binding IC<sub>50</sub>, nM (±StD, n)</b>	<b>h-sstr3 antag IC<sub>50</sub>, nM (±StD, n)</b>	<b>hERG binding IC<sub>50</sub>, μM (n)</b>
5	0.8 (0.3, 5)	26.1 (nd, 1)	0.08 (2)
9	11.3 (7.2, 3)	28.1 (20.2, 2)	0.20 (2)
10	20.0 (3.9, 4)	28.6 (1.3, 2)	0.19 (2)
11	11.5 (7.0, 4)	17.2 (12.7, 2)	0.09 (2)
12	53.3 (nd, 1)	134.6 (45.3, 2)	0.34 (2)
13	2.6 (0.5, 2)	4.8 (nd, 1)	0.17 (2)
14	3.0 (0.7, 17)	2.5 (2.1, 4)	8.54 (4)

<sup>a</sup>StD = standard deviation; *n* = number of determinations; nd = not determined.

have hERG activity.<sup>8</sup> An exploration of imidazole substitution and replacement, including *N*-methylation, iso-imidazolyl, isoxazolyl, and oxadiazolyl, was not fruitful and will be reported separately. The three pyridyl isomers 9, 10, and 11 afforded a loss of sstr3 binding relative to the phenyl analogue 5 but generally retained similar antagonist activities. Changes to hERG channel binding were modest. The pyrazine analogue 12 offered no advantages in terms of potency or selectivity. The addition of a 4-fluoro substituent had previously been shown to increase sstr3 potency and was added to the 2-pyridyl group in 9 to afford 13, which seemed to improve selectivity of receptor antagonism vs hERG activity.<sup>1</sup> The 4-fluoro-2-pyridyl moiety was incorporated into 1 to afford 14, which again only showed a modest improvement in hERG selectivity. Compound 14 had a similar profile to 1 in the mouse oGTT model (~82% inhibition at 1 mg/kg po). In a patch clamp assessment of hERG activity, 14 afforded an IC<sub>50</sub> = 12 μM (IC<sub>20</sub> ≈ 3 μM),<sup>9</sup> representing a 3–4-fold improvement over 1. Unfortunately, 14 also exhibited a greater increase in the QTc interval in dogs than 1 at similar plasma concentrations. Clearly a 3–4-fold improvement in hERG activity was insufficient to minimize or eliminate the QTc prolongation.

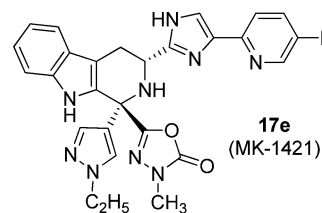
In the discovery phase of **1** (MK-4256), it was found that hERG channel binding could be greatly reduced by placement of a variety of heteroaryls at the C-1 position of the tetrahydro- $\beta$ -carboline scaffold.<sup>1</sup> In particular, substituted pyrazoles and oxadiazoles afforded an attractive balance between sstr3 potencies, pharmacokinetic profiles, and off-target activities. The effect of simple substitution on the pyrazole and 1,2,4-oxadiazole rings is shown in Table S1 (see Supporting Information). Compound **15a** loses some sstr3 potency, while compounds **15b–d** retain a sstr3 profile similar to that of **14**, but no improvement in hERG channel binding overall. The more polar substituents in **15e** and **15f** afford a loss of potency on the receptor.

Effects on substitution of the isomeric 1,3,4-oxadiazole analogues **16** are shown in Table S1. Simple alkyl substitution in **16a–c** afforded a similar profile to **14**. The more polar heteroatom replacements in **16d**, **16e**, and **16g** with hydroxyl, sulfhydryl, and amino, respectively, retain sstr3 potency and trend toward reduced hERG channel binding. Alkylation of the heteroatoms in **16f**, **16h**, and **16i** return hERG activity toward that of **14**. Alkylation of the hydroxyl analogue **16d** did not give O-alkylation but rather N-alkylation to afford the oxadiazolones **17**. This was a fortuitous result as these compounds generally retained sstr3 activities with much reduced hERG binding. QSAR modeling of hERG binding from Table S1 suggested a correlation with hydrophobicity (more hydrophobicity led to worse hERG), which might be addressed prospectively via PSA and cLogP (see Supporting Information). While the trends present in the data set provide a path away from low micromolar hERG binders, the statistical significance of the model indicated the need to include a more diverse compound set which would likely represent a more dynamic range in measured hERG.

The smaller alkyl substituents in **17b–e** afforded sstr3 profiles similar to **1** but with >10-fold less hERG channel activities. More importantly, these analogues reduced glucose excursion in a mouse oGTT model after oral dosing at 1 mg/kg po. The only slightly larger alkyl groups in **17i–j** once again brought back too much hERG binding. The dimethylaminoethyl derivative **17k** also had significant hERG activity, whereas the acid **17l** and amide **17m** both had reduced ion channel binding but lost efficacy in the mouse oGTT evaluation. Both **17c** and **17e** had comparable profiles, but in a functional patch clamp hERG assay, the former compound afforded an  $IC_{50} = 12 \mu\text{M}$  vs  $27 \mu\text{M}$  for **17e**. Given its superior profile, compound **17e** was chosen as a potential development candidate.

The configuration of **17e** was determined to be (1*R*,3*R*) by <sup>1</sup>H NMR (nOE) analysis of starting material **16d**; the 3*R* position was assigned from the starting material D-tryptophan.<sup>10,11</sup> The (1*S*,3*R*) diastereomer **17f** and the (1*S*,3*S*) isomer **17g** were 10–100-fold less potent as an sstr3 antagonist compared to **17e**. The binding profile of **17e** vs sstr3 from other species and the other human sstr subtypes is shown in Table 4. These data clearly show that **17e** is very potent vs sstr3 from other preclinical species and is highly subtype selective. No agonist activity was noted for any sstr subtype (data not shown).

Additional evaluation of off-target hits is shown in Table 5. Selectivity vs ion channels, CYPs, and a screening panel of 150 enzyme and receptor targets was excellent as was the lack of activity against PXR activation. Acceptable time-dependent inhibition of CYP3A4 was noted.

Table 4. In Vitro Binding Profile of **17e**<sup>a</sup>

Potencies of <b>17e</b> vs sstr3 from other species				
$IC_{50}$ , nM (( $\pm$ StD, n))				
human	mouse	rat	dog	rhesus
2.3 (0.9, 23)	1.3 (0.3, 4)	0.6 (0.1, 2)	2.5 (1.0, 4)	1.0 (0.3, 2)
Selectivity of <b>17e</b> vs the other human sstr subtypes				
$IC_{50}$ , nM (( $\pm$ StD, n))				
sstr1	sstr2	sstr3	sstr4	sstr5
5776 (585, 4)	>10 <sup>4</sup>	2.3 (0.9, 23)	>10 <sup>4</sup>	9240 (316, 3)

<sup>a</sup>StD = standard deviation; n = number of determinations; nd = not determined.

Table 5. Off-Target Profile of **17e**

Ion channels		
hERG (MK-499 binding)	$IC_{50}$ , $\mu\text{M}$	32.2
hERG (PatchExpress)	$IC_{50}$ , $\mu\text{M}$	27
I <sub>Ks</sub>	$IC_{50}$ , $\mu\text{M}$	>30
NaV <sub>1.5</sub>	$IC_{50}$ , $\mu\text{M}$	>30
CaV <sub>1.2</sub>	$IC_{50}$ , $\mu\text{M}$	>30
CYPs 2C8, 2C9, 2D6, 3A4	$IC_{50}$ , $\mu\text{M}$	>10
CYP3A4 time dependent inhibition	(min <sup>-1</sup> )	0.011
PXR	$EC_{50}$ , $\mu\text{M}$	>30
PanLabs screen (hits 1-10 $\mu\text{M}$ )		4 / 150
Screening hits:	$IC_{50}$ , $\mu\text{M}$	PDE <sub>4</sub> 5.65 NK <sub>2</sub> 4.28 sstr <sub>1</sub> 1.33 sstr <sub>5</sub> 1.53

The pharmacokinetic profile in four preclinical species is listed in Table 6. Bioavailability was poor in rodent species but much better in higher species. This compound is an efficient substrate for the transporter P-glycoprotein (PGP) in several

Table 6. Pharmacokinetic Profile and Plasma Protein Binding (PPB) of **17e** in Preclinical Species<sup>a</sup>

	Pharmacokinetics				PPB	
	Cl <sub>p</sub> (mL/min/kg)	V <sub>dss</sub> (L/kg)	t <sub>1/2</sub> (hr)	F (%)	F <sub>u</sub> (%)	
mouse	27	2.8	1.2	9	8.4	
rat	48	3.4	1.2	2	14.5	
dog	5.3	1.3	3.2	100	14.4	
rhesus	5.3	1.4	2.7	40	7.4	
human					9.8	

<sup>a</sup>Cl<sub>p</sub> = plasma clearance; V<sub>dss</sub> = volume of distribution at steady state; t<sub>1/2</sub> = plasma half-life after iv dosing; F = oral bioavailability; F<sub>u</sub> = unbound fraction determined in vitro.

species (BA/AB: mouse 19; rat 16; human 31).<sup>12</sup> As a consequence, brain penetration is very low (brain/plasma concentration ratio b/p = 0.02; see Supporting Information).<sup>12</sup> The compound also exhibits poor permeability with a permeability coefficient  $P_{app} < 10 \text{ cm} \cdot 10^{-6} / \text{sec}$ . The combination of PGP transport and low permeability may explain the poor bioavailability in rodents. Plasma protein binding is comparable among all species.

Compound **17e** was assessed for its ability to improve glucose tolerance in lean C57BL/6N mice. Oral administration of **17e** 1 h prior to dextrose challenge in an oral glucose tolerance test (oGTT) significantly reduced blood glucose excursion in a dose-dependent manner from 0.03 to 3 mg/kg (Figure 1). The cumulative results from separate titrations

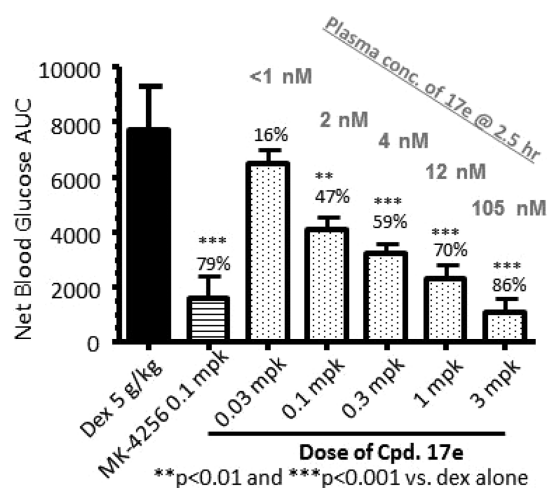


Figure 1. Titration of **17e** in mouse oGTT.

demonstrated that at 3 mg/kg inhibition was near 100%. The plasma levels of **17e** determined at the completion of the oGTT study ( $\sim 2.5$  h post dose) were 1, 2, 4, 12, and 105 nM at 0.03, 0.1, 0.3, 1, and 3 mg/kg po, respectively. The  $ED_{50}$  for **17e**-induced suppression of oGTT glucose levels in mouse was 0.16 mg/kg, and the  $MED_{max}$  (minimal efficacious dose for maximal suppression of blood glucose during oGTT) was 3 mg/kg po. The effect of **17e** on insulin release in the presence of low and high glucose concentrations in isolated human islets was examined. As shown in Figure 2, compound **17e** ( $5 \mu\text{M}$ ) augmented insulin secretion at 16 mM glucose, but not at 2 mM glucose during a 60 min static incubation of human islets from two nondiabetic donors. Compound **17e** did not affect the release of glucagon nor somatostatin (SS-14) at either glucose concentrations (data not shown). GLP-1 (50 nM) and linoleic acid (100  $\mu\text{M}$ ) were used as positive controls for insulin/somatostatin and glucagon release, respectively.

In light of the cardiovascular issues associated with compound **1**, the potential of **17e** to elicit any CV effects was evaluated. Compound **17e** was administered by iv infusion to anesthetized vagus-intact dogs at various doses to achieve plasma concentrations ( $C_{max}$ ) of 17, 43, and 140  $\mu\text{M}$ .<sup>13</sup> There were no changes to any electrophysiologic parameters, including no prolongation of the QTc interval. Subsequent studies with **17e** in oral, telemetrized cardiovascular dogs revealed no significant changes ( $C_{max} = 5.8 \mu\text{M}$ ).<sup>14</sup> As a result, **17e** was chosen as an early development candidate and designated as MK-1421.

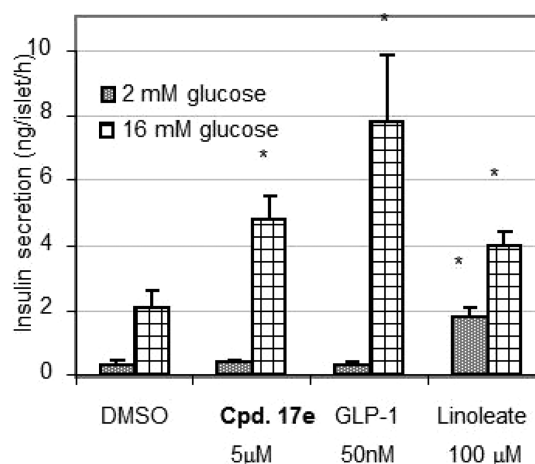


Figure 2. Insulin secretion from human islets induced by **17e**, GLP-1, and linoleic acid.

In summary, we disclose the discovery and profile of a potent, selective *ssr3* antagonist (**17e**, MK-1421) that showed excellent efficacy in a mouse model of glucose excursion (oGTT) and demonstrated glucose-dependent release of insulin from relevant human tissue. This compound has an acceptable preclinical pharmacokinetic profile. Unlike a previous candidate, **17e** demonstrated little potential for cardiovascular effects. It was chosen for further development as a potential treatment for type 2 diabetes mellitus. Further information regarding its clinical profile will be reported in due course.

## ■ ASSOCIATED CONTENT

### 📄 Supporting Information

Synthetic methods and characterization of key compounds are described along with protocols for biological assays. Table S1 is also presented. This material is available free of charge via the Internet at <http://pubs.acs.org>.

## ■ AUTHOR INFORMATION

### ✉ Corresponding Author

\*Tel: 908-723-0915. E-mail: [wkhagmann@yahoo.com](mailto:wkhagmann@yahoo.com).

### 📄 Notes

The authors declare no competing financial interest.

## ■ ACKNOWLEDGMENTS

The authors thank Li-Kang Zhang at the Merck Research Laboratories for measuring the high resolution mass of **17e**.

## ■ REFERENCES

- (1) He, S.; Ye, Z.; Truong, Q.; Shah, S.; Du, W.; Guo, L.; Dobbelaar, P. H.; Lai, Z.; Liu, J.; Jian, T.; Qi, H.; Bakshi, R. K.; Hong, Q.; Dellureficio, J.; Pasternak, A.; Feng, Z.; deJesus, R.; Yang, L.; Reibarkh, M.; Bradley, S. A.; Holmes, M. A.; Ball, R. G.; Ruck, R. T.; Huffman, M. A.; Wong, F.; Samuel, K.; Reddy, V. B.; Mitelman, S.; Tong, S.; Chicchi, G.; Tsao, K.-L.; Trusca, D.; Wu, M.; Shao, Q.; Trujillo, M. E.; Eiermann, G. J.; Li, C.; Zhang, B.; Howard, A. D.; Zhou, Y.-P.; Nargund, R. P.; Hagmann, W. K. The discovery of MK-4256, a potent SSTR3 antagonist as a potential treatment of type-2 diabetes. *ACS Med. Chem. Lett.* **2012**, *3*, 484–489.
- (2) He, S.; Lai, Z.; Ye, Z.; Dobbelaar, P.; Shah, S. K.; Truong, Q.; Du, W.; Guo, L.; Liu, J.; Jian, T.; Qi, H.; Bakshi, R. K.; Hong, Q.; Dellureficio, J.; Reibarkh, M.; Samuel, K.; Reddy, V. B.; Mitelman, S.; Tong, S. X.; Chicchi, G. G.; Tsao, K.-L.; Trusca, D.; Wu, M.; Shao, Q.

Trujillo, M. E.; Fernandez, G.; Nelson, D.; Bunting, P.; Kerr, J.; Fitzgerald, P.; Morissette, P.; Volksdorf, S.; Eiermann, G. J.; Li, C.; Zhang, B.; Howard, A. D.; Zhou, Y.-P.; Nargund, R. P.; Hagmann, W. K. Investigation of cardiovascular effects of tetrahydro- $\beta$ -carboline sstr3 antagonists. *ACS Med. Chem. Lett.* **2014**, *5*, 748–753.

(3) Cavalli, A.; Poluzzi, E.; Fabrizio De Ponti, F.; Recanatini, M. Toward a pharmacophore for drugs inducing the long QT syndrome: insights from a CoMFA study of HERG K<sup>+</sup> channel blockers. *J. Med. Chem.* **2002**, *45*, 3844–3853.

(4) Sanguinetti, M. C.; Mitcheson, J. S. Predicting drug-hERG channel interactions that cause acquired long QT syndrome. *Trends Pharmacol. Sci.* **2005**, *26* (3), 119–124.

(5) Jamieson, C.; Moir, E. M.; Rankovic, Z.; Wishart, G. Medicinal chemistry of hERG optimizations: highlights and hang-ups. *J. Med. Chem.* **2006**, *49*, 5029–5046.

(6) Poitout, L.; Roubert, P.; Contour-Galceran, M.; Moinet, C.; Lannoy, J.; Pommier, J.; Plas, P.; Bigg, D.; Thurieau, C. Identification of potent non-peptide somatostatin antagonists with sst3 selectivity. *J. Med. Chem.* **2001**, *44*, 2990–3000.

(7) Pasternak, A.; Feng, Z.; deJesus, R.; Ye, Z.; He, S.; Dobbelaar, P. H.; Bradley, S. A.; Chicchi, G. G.; Tsao, K.; Trusca, D.; Eiermann, G. J.; Feng, Y.; Wu, M.; Shao, Q.; Zhang, B.; Nargund, R. P.; Mills, S. G.; Howard, A. D.; Yang, L.; Zhou, Y.-P. Stimulation of glucose-dependent insulin secretion by a potent, selective sst3 antagonist. *ACS Med. Chem. Lett.* **2012**, *3*, 289–293.

(8) Blum, C. A.; Zhang, X.; De Lombaert, S. Design, synthesis, and biological evaluation of substituted 2-cyclohexyl-4-phenyl-1H-imidazoles: potent and selective neuropeptide Y Y5-receptor antagonists. *J. Med. Chem.* **2004**, *47*, 2318–2325.

(9) QTc interval prolongation may be observed in the guinea pig when free plasma concentrations are 3-fold the hERG IC<sub>20</sub>. This Letter also shows that the GP results translate well to non-rodents and to the clinic. Morissette, P.; Nishida, M.; Trepakova, E.; Imredy, J.; Lagrutta, A.; Chaves, A.; Hoagland, K.; Lei Hoe, C.-M.; Zrada, M. M.; Travis, J. J.; Zingaro, G. J.; Gersenser, P.; Friedrichs, G.; Salata, J. J. The anesthetized guinea pig: An effective early cardiovascular derisking and lead optimization model. *J. Pharmacol. Toxicol. Methods* **2013**, *68*, 137–149.

(10) Ernst, R. R.; Bodenhausen, B.; Wokaun, A. *Principles of Nuclear Magnetic Resonances in One or Two Dimensions*; Oxford University Press: Oxford, U.K., 1992.

(11) Neuhaus, D.; Williamson, M. P. The Nuclear Overhauser Effect in Structural and Conformational Analysis. In *Methods in Stereochemical Analysis*, 2nd ed.; Marchand, A. P., Ed.; John A. Wiley and Sons: New York, 2000.

(12) He, H.; Lyons, K. A.; Yao, Z.; Bleasby, K.; Chan, G.; Hafey, M.; Li, X.; Salituro, G. M.; Cohen, L. H.; Tang, W. Utility of unbound plasma drug levels and P-glycoprotein transport data in prediction of central nervous system exposure. *Xenobiotica* **2009**, *39*, 687–693.

(13) Tashibu, H.; Miyazaki, H.; Aoki, K.; Akie, Y.; Yamamoto, K. QT PRODACT: in vivo QT assay in anesthetized dog for detecting the potential for QT interval prolongation by human pharmaceuticals. *J. Pharmacol. Sci.* **2005**, *99*, 473–486.

(14) Toyoshima, S.; Kanno, A.; Kitayama, T.; Sekiya, K.; Nakai, K.; Haruna, M.; Mino, T.; Miyazaki, H.; Koji Yano, K.; Yamamoto, K. QT PRODACT: in vivo QT assay in the conscious dog for assessing the potential for QT interval prolongation by human pharmaceuticals. *J. Pharmacol. Sci.* **2005**, *99*, 459–471.